Automatic Delineation of Grounding Lines from Differential InSAR along the Getz Ice Shelf, Antarctica, using a Machine Learning Algorithm

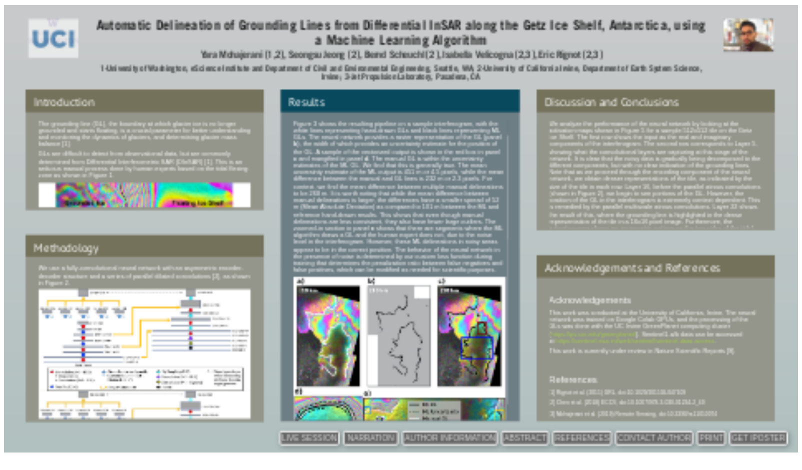

Yara Mohajerani [1,2], Seongsu Jeong [2], Bernd Scheuchl [2], Isabella Velicogna [2,3], Eric Rignot [2,3]

1-University of Washington, eScience Institute and Department of Civil and Environmental Engineering, Seattle, WA; 2-University of California Irvine, Department of Earth System Science, Irvine; 3-Jet Propulsion Laboratory, Pasadena, CA

PRESENTED AT:

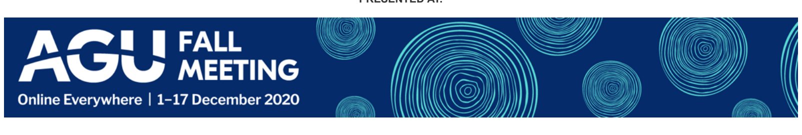

INTRODUCTION

The grounding line (GL), the boundary at which glacier ice is no longer grounded and starts floating, is a crucial parameter for better understanding and monitoring the dynamics of glaciers, and determining glacier mass balance [1].

GLs are difficult to detect from observational data, but are commonly determined from Differential Interferometric SAR (DInSAR) [1]. This is an arduous manual process done by human experts based on the tidal flexing zone as shown in Figure 1.

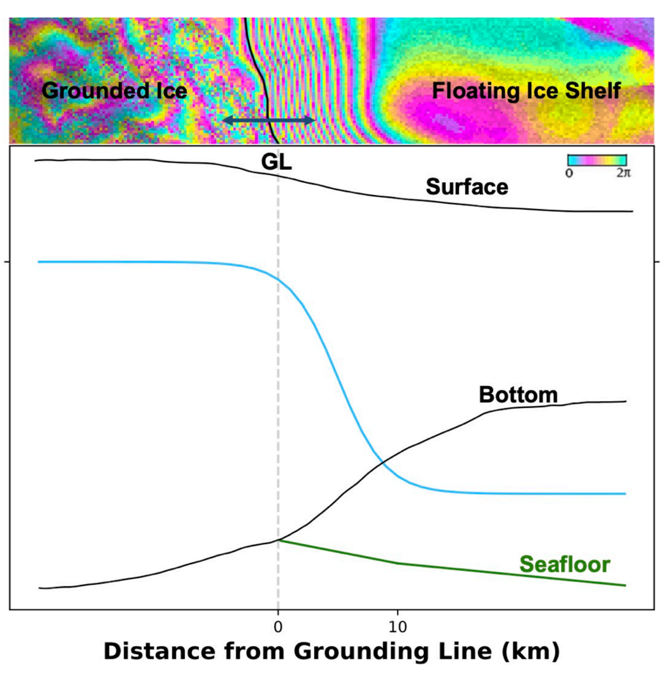

Fig1. The correspondence between a sample DInSAR interferogram and the grounding zone. The grounding line corresponds to the inner-most tidal flexing fringe.

The time-consuming nature of this manual processes is a bottleneck in large-scale monitoring of grounding lines and therefore a better understanding of glacier dynamics over time.

Here we showase a machine-learning (ML) driven framework for the automatic delineation of grounding lines, resulting in the delineation of all available Antacrctic coastline data from Sentinel1-a/b in 2018. We discuss some implications on the Getz Ice Shelf.

METHODOLOGY

We use a fully-convolutional neural network with an asymmetric encoder-decoder structure and a series of parallel dilated convolutions [2], as shown in Figure 2.

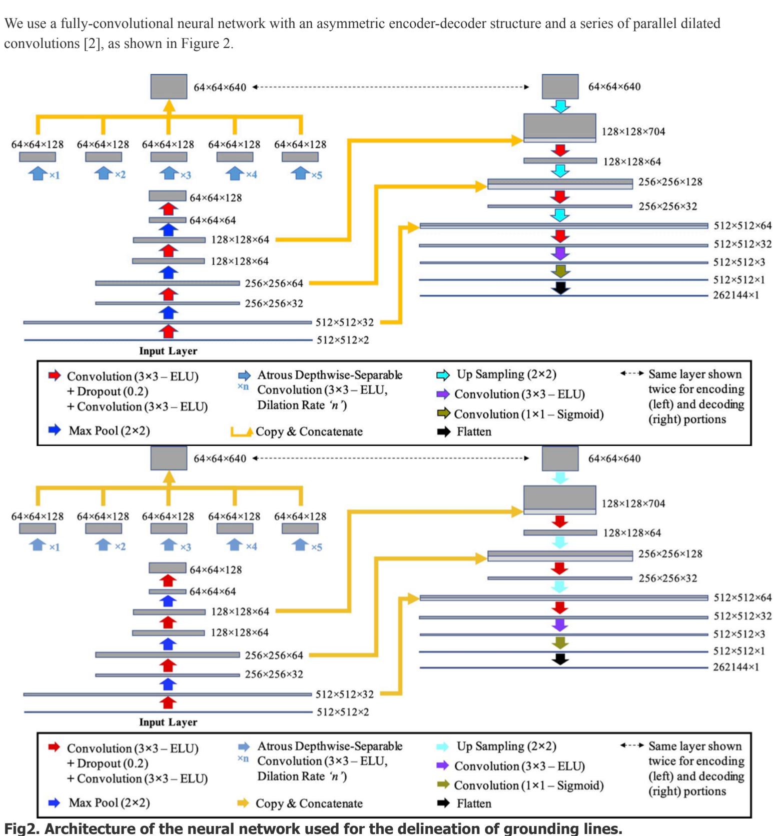

Fig2. Architecture of the neural network used for the delineation of grounding lines.

The interferograms have a considerable amount of noise and also contain features at multiple spatial scales that are relevant to finding the position of the GL. Therefore, while similar work on calving fronts and optimal imagery [3] used a simpler architecture, we find that using a deeper encoding component and including a series of parallel multi-scale convolutions as depth-wise separable atrous convolutions [4,5] provides significant improvements to GL delineations.

Interferograms are divided into partially overlapping tiles that are 512 x 512 pixels, with each pixel having a resolution of 100 m. The network is trained on 5,320 tiles, 520 of which are used for validation while training to avoid overfitting. The corresponding hand-drawn GLs are used as training labels.

RESULTS

Figure 3 shows the resulting pipeline on a sample interferogram, with the white lines representing hand-drawn GLs and black lines representing ML GLs. The neural network provides a raster representation of the GL (panel **b**), the width of which provides an uncertainty estimate for the position of the GL. A sample of the vectorized output is shown in the red box in panel **c** and mangified in panel **d**. The manual GL is within the uncertainty estimates of the ML GL. We find that this is generally true. The mean unceraity estimate of the ML output is 451 m or 4.5 pixels, while the mean difference between the manual and GL lines is 232 m or 2.3 pixels. For context, we find the mean difference between multiple manual delineations to be 268 m. It is worth noting that while the mean difference between manual delineations is larger, the differences have a smaller spread of 52 m (Mean Absolute Deviation) as compared to 101 m between the ML and reference hand-drawn results. This shows that even though manual delineations are less consistent, they also have fewer large outliers. The zoomed-in section in panel **e** shows that there are segments where the ML algorithm draws a GL and the human expert does not, due to the noise level in the interferogram. However, these ML delineations in noisy areas appear to be in the correct position. The behavior of the neural network in the presence of noise is determined by our custom loss function during training that determines the penalization ratio between false negatives and false positives, which can be modified as needed for scientific purposes.

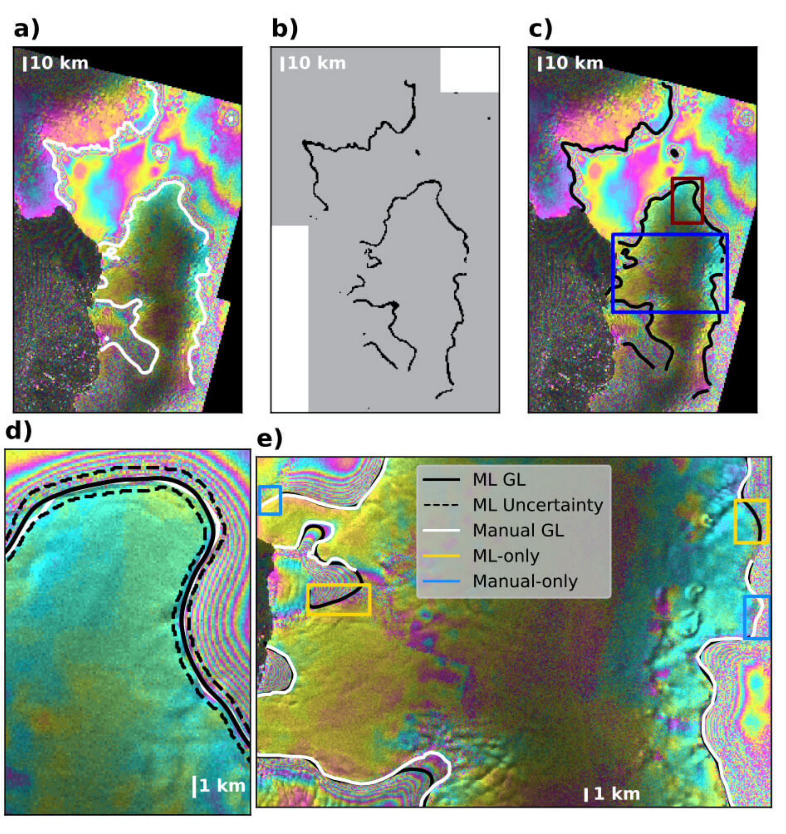

Fig3. Results of the ML pipeline for a sample interferogram. Manual delineations are in white and ML delineations are in black.

Finally, we apply the pipeline to all available differential InSAR data with 6-day and 12-day intervals around the Antarctic coastline from Sentinel1-a/b during 2018, as shown in panel **b** of Figure 4 [6,7]. This totals to 22,935 interferograms or 4,507,501 512x512 tiles. With the trained network, delineating the entire coastline takes about 21 hours of GPU (Graphical Processing Unit) time, whereas it would take 7,600 hours of manual work for the same effort. The results of the delineation are shown in panel **a** of Figure 4. The complete dataset will be made accessible [8].

The zoomed-in area in panels **c** and **d** focus on a section of the West Antarctic coastline. Changes in the position of the grounding line throughout the year can be seen in panel **c**. Importantly, we see that this range is larger than the corresponding uncertainty estimtes, as shown by three samples lines from the beginning, middle, and end of the year in panel **d**. In other words, the uncertainty is small enough to retrieve meaningful estimates of the width of the grounding zone.

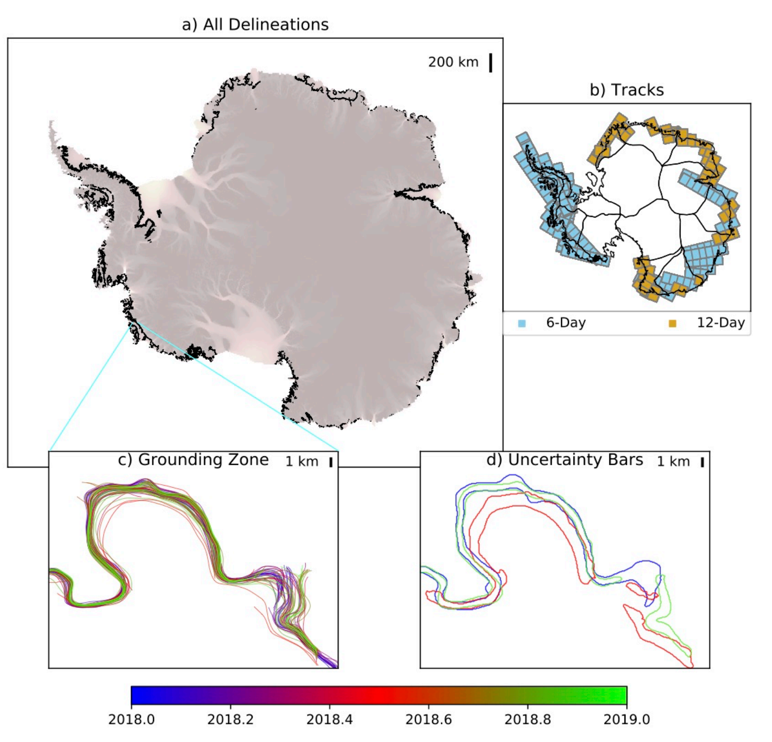

Fig4. GL delineations from all 6-day and 12-day DInSAR data from Sentinel1-a/b in 2018 (panels a,b). Zoomed-in plot (c) and corresponding uncertainty estimates (d) show changes in the position of the grounding line over time, which are larger than the uncertainty estimates of the individual lines.

DISCUSSION AND CONCLUSIONS

We analyze the performance of the neural network by looking at the activation maps shown in Figure 5 for a sample 512x512 tile on the Getz Ice Shelf. The first row shows the input as the real and imaginary components of the interferogram. The second row corresponds to Layer 5, showing what the convolutional layers are capturing at this stage of the network. It is clear that the noisy data is gradually being decomposed to the different components, but with no clear indication of the grounding lines. Note that as we proceed through the encoding component of the neural network, we obtain denser representations of the tile, as indicated by the size of the tile in each row. Layer 16, before the parallel atrous convolutions (shown in Figure 2), we begin to see portions of the GL. However, the position of the GL in the interferogram is extremely context dependent. This is remedied by the parallel multiscale atrous convolutions. Layer 22 shows the result of this, where the grounding line is highlighted in the dense representation of the tile in a 16x16 pixel image. Furthermore, the activation map shows an asymmetric pattern on the two sides of the tidal flexing zone, clearly distinguishing the two sides from contextual information. This is key to labelling the correct side of the flexing zone as the GL.

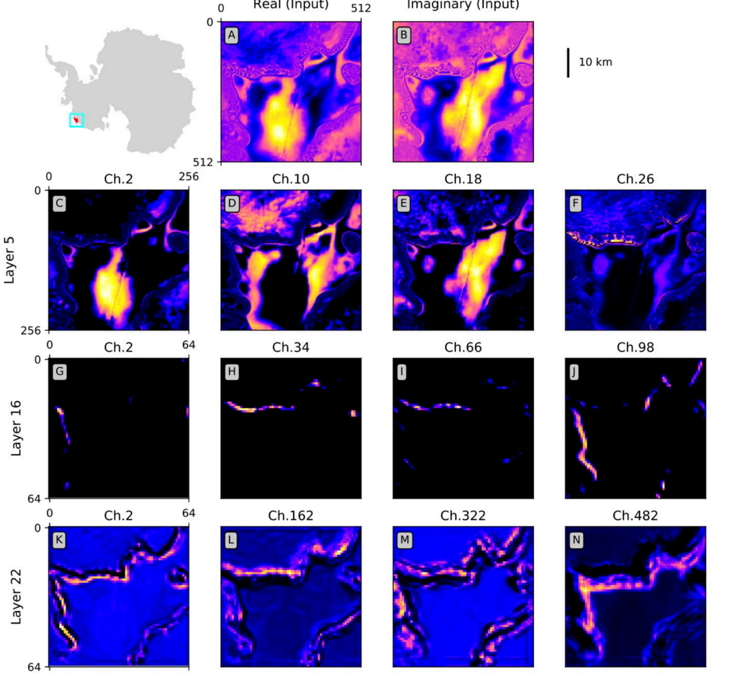

Fig5. Activation maps showing what is being detected by the convolutional kernels at different stages of the neural network. The importance of multi-scale atrous convolutions is highlighted in the last row.

Comprehensive delineation of grounding lines allows us to quantify the width of the grounding zone, the area over which the grounding line migrates with the tides. Observational data on the position of the grounding line and the width of the grounding zone on a large scale that includes the entire ice sheet provide new insights on the dynamics of the grounding zone that can better inform modelers of the evolution of marine-terminating glaciers.

ACKNOWLEDGEMENTS AND REFERENCES

Acknowledgements

This work was conducted at the University of California, Irvine. The neural network was trained on Google Colab GPUs, and the processing of the GLs was done with the UC Irvine GreenPlanet computing cluster (https://ps.uci.edu/greenplanet/). Sentinel1-a/b data can be accessed at https://sentinel.esa.int/web/sentinel/sentinel-data-access.

This work is currently under review in Nature Scientific Reports [9].

References

[1] Rignot et al. (2011) GRL, doi:10.1029/2011GL047109

[2] Chen et al. (2018) ECCV, doi:10.1007/978-3-030-01234-2_49

[3] Mohajerani et al. (2019) Remote Sensing, doi:10.3390/rs11010074

[4] Chen et al. (2017) arXiv:1706.05587

[5] Chollet (2016) arXiv:1610.02357

[6] Geudtner et aL (2012) Proceedings of the 9th European Conference on Synthetic Aperture Radar, Nürnberg, Germany, 23–26.

[7] Torres et al. (2012) Remote. Sens. Environ., doi:10.1016/j.rse.2011.05.028

[8] Mohajerani et al. (2020) UC Irvine, Dataset, doi:10.7280/D1VD6G

[9] Mohajerani, Y., Jeong, S., Scheuchl, B., Velicogna, I., Rignot, E. (2020) "Automatic Delineation of Glacier Grounding Lines with Differential Interferometric Synthetic-Aperture Radar and Deep Learning", Nature Scientific Reports, **in review**.

AUTHOR INFORMATION

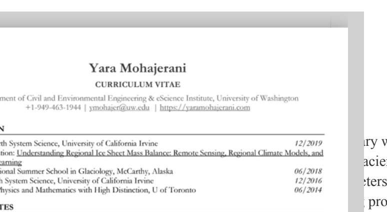
Yara Mohajerani
CURRICULUM VITAE
Department of Civil and Environmental Engineering & eScience Institute, University of Washington
+1-949-463-1944 | ymohajer@uw.edu | https://yaramohajerani.com
EDUCATION
- Ph.D. in Earth System Science, University of California Irvine 12/2019
  - Dissertation: Understanding Regional Ice Sheet Mass Balance: Remote Sensing, Regional Climate Models, and Deep Learning
  - International Summer School in Glaciology, McCarthy, Alaska 06/2018
- M.S. in Earth System Science, University of California Irvine 12/2016
- H.B.Sc. in Physics and Mathematics with High Distinction, U of Toronto 06/2014

CERTIFICATES

...ry where glacier ice is no longer supported by the ... acier dynamics and better quantification of glacier ... eters from Differential Interferometric Synthetic ... process that is not scalable for large-scale delineation from the ever-larger amount of remote-sensing data becoming available, which is necessary for a better understanding of glaciological processes. In order to solve this issue, we present a deep learning approach using a convolutional neural network with parallel atrous convolutions and an asymmetric encoding/decoding structure to successfully delineate thousands of grounding lines rapidly and accurately. Furthermore, the neural network outputs uncertainty estimates, which have so far been missing from grounding line delineations. Over the Getz Ice Shelf in West Antarctica, we find a mean difference of 232 meters, or 2.3 pixels, between automatic delineations and manual delineations on test data not used during training. The spread of differences is given by a median absolute deviation of 101 meters. The performance of the neural network is comparable to that of human interpreters, with manual delineations falling within the uncertainty range of automatic delineations. Similar differences exist between multiple manual delineations, with a slightly higher mean difference (268 meters) and a lower spread (median absolute deviation of 52 meters). We show our deep learning pipeline is easily generalizable and scalable to the entire ice sheet, revolutionizing the availability of grounding line delineations for glaciological studies.

REFERENCES

[1] Rignot et al. (2011) GRL, doi:10.1029/2011GL047109

[2] Chen et al. (2018) ECCV, doi:10.1007/978-3-030-01234-2_49

[3] Mohajerani et al. (2019) Remote Sensing, doi:10.3390/rs11010074

[4] Chen et al. (2017) arXiv:1706.05587

[5] Chollet (2016) arXiv:1610.02357

[6] Geudtner et aL (2012) Proceedings of the 9th European Conference on Synthetic Aperture Radar, Nürnberg, Germany, 23–26.

[7] Torres et al. (2012) Remote. Sens. Environ., doi:10.1016/j.rse.2011.05.028

[8] Mohajerani et al. (2020) UC Irvine, Dataset, doi:10.7280/D1VD6G

[9] Mohajerani, Y., Jeong, S., Scheuchl, B., Velicogna, I., Rignot, E. (2020) "Automatic Delineation of Glacier Grounding Lines with Differential Interferometric Synthetic-Aperture Radar and Deep Learning", Nature Scientific Reports, **in review**.